Induced seismicity, well azimuth, and completion economics in the Duvernay

Scott McKean[1] and Suzie Jia[1]

[1] Schulich School of Engineering, University of Calgary, Calgary, Alberta, Canada T2N 1N4; Tel.: +1 403-700-5883; scott.mckean@ucalgary.ca, suzie.jia@ucalgary.ca

Key Words: induced seismicity, Duvernay formation, fault slip potential, drilling and completion, geomechanics, wellbore stability, wellbore azimuth, statistical analysis

Abstract:

Induced seismicity is a major challenge for the Canadian energy sector, especially in the Duvernay Formation. This study uses the Mohr-Coulomb criterion to investigate induced seismicity mechanisms, which principally consist of hydraulic and total stress perturbations. It proposes two structural models for optimally oriented faults and shows that faults in the Duvernay are very sensitive to triggering. It then looks at the influence of wellbore azimuth on wellbore stability, induced seismicity, operations, and economics – both theoretically and through a statistical comparison of north south and diagonal laterals in the Kaybob area of the Duvernay. The study argues that the presence of north-south wells may exacerbate total and hydraulic stress perturbation and that it may be economically advantageous to drill wells north south as opposed to diagonally.

1.0 Introduction

Induced seismicity (IS) is a major challenge for the energy sector. We define IS as earthquakes attributable to industrial activities that are large enough to be felt at surface or register a local magnitude (M_L) above 2 on the Richter scale (Richter, 1935). Induced seismicity has many possible causes including wastewater injection, oil and gas exploitation, mining, geothermal development, carbon sequestration, and reservoir impoundment. Hitzman *et al.* (2012)

investigated a wide range of IS events and showed that oil and gas related activities (primary extraction, secondary recovery, hydraulic fracturing, and wastewater injection) have a significant potential for triggering seismicity by increasing the pore pressure in the subsurface, relative to the other causes in their study (Figure 1).

This problem is relevant to Canada, since some of the largest earthquakes attributed to hydraulic fracturing have been observed in the Devonian strata of the Horn River Basin (HRB) and the Duvernay (Ellsworth, 2013; Atkinson *et al.*, 2016). A M_L 4.44 event was triggered on August 4, 2014 in the HRB (Farahbod *et al.*, 2015). A M_L 4.36 was triggered on January 23, 2015 in the Kaybob Area of the Duvernay (Schultz *et al.*, 2015). Reef complexes control the geology of both formations and significant subvertical faults are present in both.

Operators have adjusted the azimuth of their horizontal wells (i.e. laterals) perpendicular to the maximum stress azimuth in an attempt to avoid IS and optimize production. This study investigates the effect of well azimuth on IS and production economics, specifically focusing on the Kaybob Area of the Duvernay. It reviews IS mechanisms and discusses how well orientation might affect fault stress, geomechanics, and production economics.

2.0 Background

2.1 Induced Seismicity Mechanisms

There are two fundamental ways to trigger IS through fluid injection (Figure 2) - reducing the effective stress on the fault via direct hydraulic connections and/or a changing the loading condition on the fault through poroelastic stress transmission (Healy *et al.*, 1968; Raleigh *et al.*, 1976). Mohr-Coulomb failure theory (Mohr, 1900; Labuz and Zang, 2012) is used to show why a fault will be activated once the shear stress on the fault plane exceeds the shear strength of the fault (τ_f), which is a product of the cohesion (c), the normal stress (σ_n), the pore pressure in the fault (u),

and the coefficient of friction (ϕ) (Jaeger, 1959). The Mohr-Coulomb criterion is simple, but it adequately quantifies the potential for fault reactivation.

$$\tau_f = c + (\sigma_n - u)\tan\phi \quad [1]$$

Fluid pressure decreases the effect of σ_n and thus the fault's frictional shear resistance, which provides order of magnitudes more slip resistance that its cohesion - considered negligible or at most 1 or 2 MPa (Zoback, 2010). Remote triggering of a fault is made possible due to volumetric changes in the reservoir from fluid injection. A tectonic stress regime, which is dominant in the Western Canadian Sedimentary Basin (WCSB), results in a subsurface that is nearly always critically stressed. This means that it is possible for a minor stress perturbation (1 to 5 MPa) to trigger seismicity if an optimally oriented and critically stressed fault is located near a hydraulic fracture treatment (Ellsworth, 2013).

2.2 The Duvernay Formation

The Duvernay Formation, a prolific unconventional reservoir in the WCSB, is a seminal example of a critically stressed fault regime. It is a laterally extensive anoxic and sulphidic Frasnian basin fill deposited contemporaneously with the Leduc reef buildup (Figure 3), as documented by Dunn (2012) and Rivard (2014), among others. Its geological facies include organic and clay-rich shale, massive or bioturbated limestones, and interbedded shales/limestones (Loucks 2011).

Its significant overpressure likely contributes to both the observed IS and its high productivity. In addition to high pore pressure (u), the Duvernay is also subject to high horizontal stresses (σ_H) oriented towards the northeast due to mountain building tectonics (Lele *et al.*, 2017).

Two mechanisms could generate optimally oriented faults in the Duvernay given the current combination of minimum (σ_h) and maximum (σ_H) horizontal stress. An optimal slip orientation results from a high angle or vertical fault being oriented 45 degrees (θ) to σ_H (Equations

2 and 3). This means that north-south striking faults are the most susceptible to induced seismicity in the Duvernay.

$$\tau = \frac{\sigma_h - \sigma_H}{2}\sin(2\theta) \quad [2]$$

$$\sigma_n = \sigma_h + \frac{\sigma_h - \sigma_H}{2}\cos(2\theta) \quad [3]$$

North-south faults could be generated as a result of strike-slip fractures and faults relieving tectonic stress and accommodating tectonic strain. These occur at oblique angles to the historic principal stress direction (generally 30 or 60 degrees) and a small reorientation of the tectonic could result in these faults being optimally oriented (Nelson, 2001; Maxwell, 2009). The Mesosoic orogenies (especially the Jurassic Cordilleran deformation) could easily have reoriented the modern tectonic stress regime from that present during the Paleozoic deposition of the Duvernay (Wright *et al*., 1994). The presence of the Chinchaga rift basin, which underlies the Kaybob area of the Duvernay, might also be responsible for north-south faulting. A rift basin is an extensional structure that generates high angle normal faulting as results from the combination of reef building and Precambrian basement faulting (O'Connell *et al.,* 1990). The two mechanisms and the location of the Chinchaga basin are shown in Figure 4.

3.0 Analysis

3.1 Fault Slip Potential

The fault slip potential in the Kaybob region was analyzed using the Mohr-Coulomb criterion. A range for stress gradients was obtained from Soltanzadeh *et al*. (2015) and Fox *et al.* (2015). The range for vertical stress (σ_V) was 22 to 23 MPa/km, σ_h was 19 to 23 MPa/km, σ_H was 27 to 32 MPa/km, and u was 15 to 18 MPa/km. Vertical stress was assumed to be vertical. The orientation of the maximum horizontal stress was obtained from the World Stress Map project (Heidbach et al., 2008). These orientations are interpreted from an analysis of wellbore failure mechanisms and

diagnostic fracture injection tests (DFITs) (Figure 5). The events were filtered such that only reliable (A, B, or C quality) events were used and a distribution of the σ_H azimuth obtained (Figure 6). A normal distribution approximation of the distribution yielded a mean of 45.7° with a standard deviation of 8.9°. The fault coefficient of friction (tan∅) was assumed to be 0.6 – a common practice in industry because of the difficulty and lack of studies in characterizing fault friction.

The scenario published by Lele *et al.* (2017) with c = 2 MPa, σ_V = 76.9 MPa, σ_H = 92 MPa, σ_h = 64.6 MPa, and u = 53.8 MPa is used here to exemplify the analysis results. Figure 4 shows the effect of varying fault orientations on fault slippage with cohesion. Figure 5 shows fault slippage without the 2MPa cohesion value. This example shows that it is relatively easy to trigger slip on a pre-existing fault given Lele *et al.* (2017)'s assumptions, especially when the fault cohesion is low. Faults with azimuths of 15° or 75° were most likely to be reactivated. This example shows that small perturbations in the pore pressure (which shifts the Mohr circle towards the failure surface) or total stress (which increases the radius of the Mohr circle without shifting its center) can destabilize the existing fault systems in the Kaybob area.

A bootstrap Monte-Carlo analysis was used to determine the probability of fault slip. The probability distributions specified in Table 1 were used for each of the input parameters in the Mohr-Coulomb criterion. A million trials indicated that the probability of failure was 23% without pore pressure or total stress perturbations and 29% with perturbations. This clearly shows the sensitivity of uniformly distributed faults in the Duvernay, and the probability of failure would even higher if faults had a structural preference for a north-south orientation.

3.2 Well Azimuth, Wellbore Stability, and Induced Seismicity

Anecdotal reports from Duvernay operators suggest the lateral azimuth influences the risk of IS and completions effectiveness. The preliminary results of a poll of Duvernay practitioners shows that they are divided on the issue, with a third of respondents agreeing, a third disagreeing, and a third unsure or neutral. This section investigates the effect of lateral azimuth on wellbore stability and induced seismicity.

Increased stresses around the wellbore make drilling more difficult. The Kirsh (1898) stress solution for a circular cavity, as improved by Hiramatsu and Okay (1962), was used to investigate the change in stresses and wellbore stability from changing the azimuth of a horizontal lateral. The hoop stress (σ_θ), the primary cause of wellbore failure, was calculated using Equation 4 using the stresses and wellbore fluid pressure (u_w).

$$\sigma_\theta = \sigma_H - 2(\sigma_H - \sigma_h)\cos(2\theta) - u_w \quad [4]$$

The Kirsh equations also govern the breakdown pressure required to hydraulically fracture a formation and were adopted by Hubbert and Willis (1957) to model fracture propagation. Based on these two theories, the stresses around a wellbore with different azimuths relative to σ_H were analyzed. The results, depicted in Figure 7, show that the hoop stress becomes more uniform and lessens for the north-south wells relative to the diagonal ones. This means that it should be easier to drill north south, but more difficult to complete and hydraulically fracture the formation. The fractures will also propagate obliquely to the wellbore and not perpendicularly, as expected in the diagonal laterals. It is possible that the drilling difficulty would be compensated for by the ease of completions in diagonal wells – a major implication for play economics.

We hypothesize that laterals with north south azimuths may indeed increase the likelihood and severity of induced seismicity through stress shadowing and volumetric loading of the fault.

By aligning oblique fractures with the dominant north-south fault plane, a north south lateral would be able to generate significantly more compressional loading on the fault than a diagonal one. Since fracture flow is likely to dominate Devonian poroelastic loading, the pore pressure transmission to the fault would likely be consistent between the two azimuths. So, the north south wells could create a larger compressional stress around an existing fault which would then be triggered through fracture flow. This would result in a larger and more unstable slip surface and a larger IS event, since the magnitude of induced seismicity is relative to the slip zone and stress drop (Brune, 1970), as illustrated by Brune's (1970) relationship between earthquake magnitude (M_O), fault radius (r^3), and stress drop ($\Delta\sigma$) (Equation 5).

$$M_O = \frac{16}{7}\Delta\sigma r^3 \quad [5]$$

3.3 Well Azimuths, Economics, and Operations

Public data from the Kaybob area, extracted using Geoscout®, was analyzed statistically to investigate how well azimuth affects economics and operations. Diagonal azimuths lining up perpendicular to the maximum horizontal stress were compared with north-south azimuths lined up with lease boundaries. There were 378 wells in the Kaybob area - 197 (52%) completed diagonally and 162 (43%) completed north south. Vertical wells or east west laterals were omitted.

The gas production and drilling days from each subset were compared. The observations were normalized against lateral length, which was approximated consistently by taking the measured depth of the well minus its true vertical depth. The drill days were determined by subtracting the rig release date (the date on which a rig conducted its last well operations for drilling) from the spud date (when the rig commenced drilling). The number of completion days in each subset was also compared, after normalizing by the average stage spacing. The Kolmogorov-Smirnov (KS) test for goodness of fit was used for the comparison. The KS test

assesses the confidence level (P-value) that two data sets come from different distributions (more precisely by rejecting the null hypothesis that they come from identical populations) (Massey, 1951; Razali *et al.,* 2011).

Figure 9 shows a summary of the three comparisons. The analysis indicated that there was an insignificant ($p = 0.017$) increase in diagonal gas production (20.0 m^3/day/100 m vs. 18.4 m^3/day/100 m). This is despite the significantly ($p = 1x10^{-8}$) closer stage spacing on the diagonal wells (92 m) when compared to north-south wells (117 m). The mean drilling days on north south wells (3.7 days / 100 m) was significantly ($p = 1x10^{-11}$) higher than diagonal wells (2.9 days / 100 m. The mean completion time for both subsets (0.52 days / stage for diagonals vs. 0.48 days / stage for north-south wells) was close, but they followed significantly different distributions. These results contradict some empirical rules held by industry. We can't statistically prove that diagonals are better producers than north-south wells. The drilling time contradicts our above geomechanical analysis, which indicates that it should be easier to drill a well north south because of lower hoop stresses. Additionally, diagonal wells took longer to complete than north-south wells, despite anecdotal evidence from operators to the contrary. A full economic analysis isn't possible because of varying operator expertise and formation heterogeneity, but the results support the use of north south wells in field development.

The impact of north south deployment can be demonstrated with a simple drainage model based on the spacing of multi-well pads. The north south laterals had a mean spacing of 274 m with a standard deviation of 76 m and the diagonal laterals had a mean spacing of 294 m with a standard deviation of 132 m. Given their similarity, a consistent spacing of 285 m was assumed. Laterals generally cannot extend further then the true vertical depth of the well. For the Kaybob area, this results in a maximum lateral length of roughly 3 km. There are also operational limits to

the maximum number of wells on a pad, since extending the east-west doglegs increases costs and reduced lateral length. This generally limits each well pad to four laterals, which corresponds with the existing Kaybob completions. Assuming a 4-section lease ownership (3.2 km x 3.2 km), a diagonal completion would reduce the drainage area from 9.4 km^2 to 7.0 km^2 – a 25% decrease in reserves and production. The capital inputs for both scenarios will be similar, with the same land cost, three well pads, and eleven build sections (Figure 8). The only cost savings would be total lateral length reduction, from 33 km for north south development to 25 km for diagonal completion. These would at most save 10% to 15%, resulting in a net internal rate of return (IRR) reduction of at least 10%.

4.0 Conclusion

This study investigated induced seismicity mechanisms and the effect of lateral azimuth on wellbore stability, economics, and completions in the Duvernay Formation. It made the following conclusions:

- Optimally oriented faults are very sensitive to pore-pressure perturbations
- There are structural models that can explain the existence of these faults
- The presence of north-south wells may exacerbate total and hydraulic stress perturbation
- It may be economically advantageous to drill wells north-south

This leaves practitioners with a conundrum: mitigating an increased risk of induced seismicity while capturing the operational benefits of drilling north-south wells.

5.0 Tables and Figures

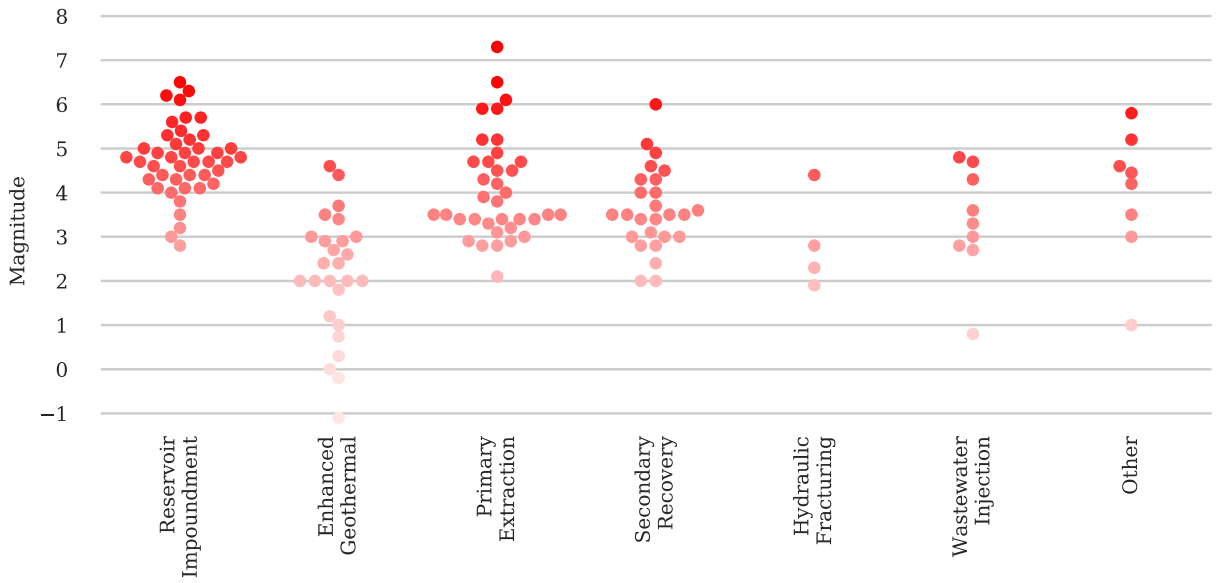

Figure 1. A bee swarm plot of the results from the National Research Council (2012) study on induced seismicity, which shows the documented magnitude of induced events by attributed cause. Note that the data is limited to events prior to 2011 (Hitzman, 2012).

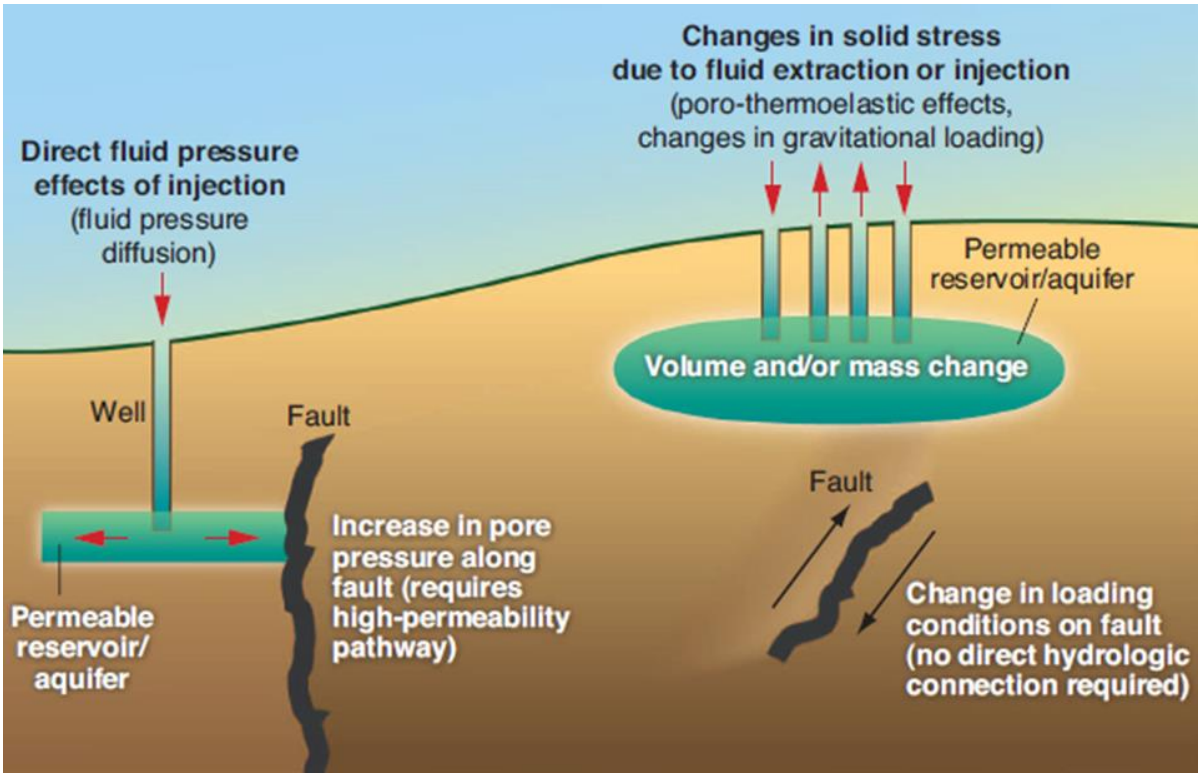

Figure 2. An illustration showing the mechanisms of induced seismicity. A direct hydraulic connection to the fault is shown on the left, where fluid pressure lubricates the fault and reduces effective stress. Remote triggering due to elastic stress changes shown on the right, where no direct hydraulic connection is established but the loading conditions change. Adapted from Ellsworth (2013).

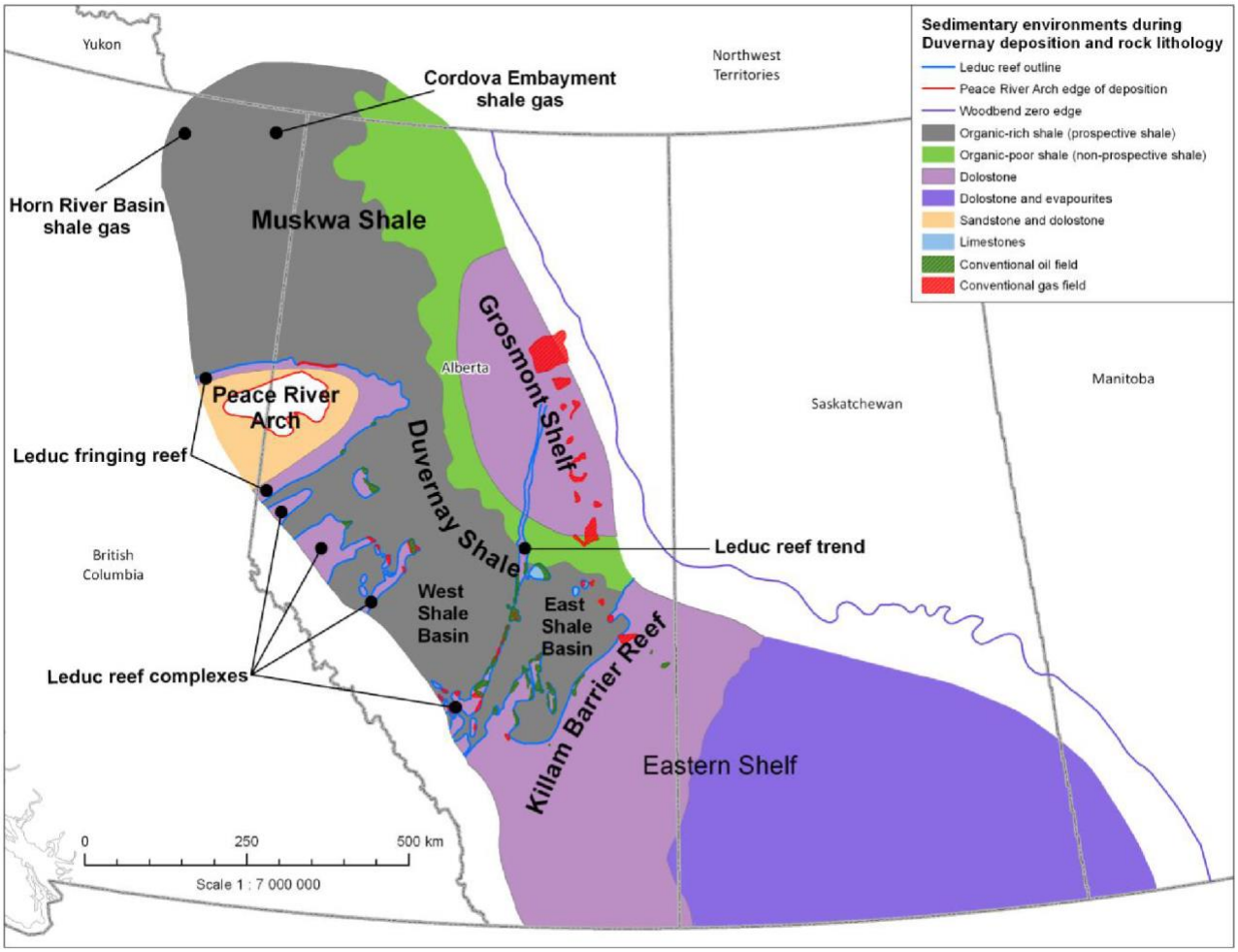

Source: Modified from Atlas of the Western Canada Sedimentary Basin

Figure 3. An illustration showing the deposition setting and geology of the Duvernay Formation. The Dolostone reefs of the Leduc reef are shown in pink. The organic rich basinal shale deposits of the Duvernay are shown in grey. Reproduced with permission from National Energy Board (2017).

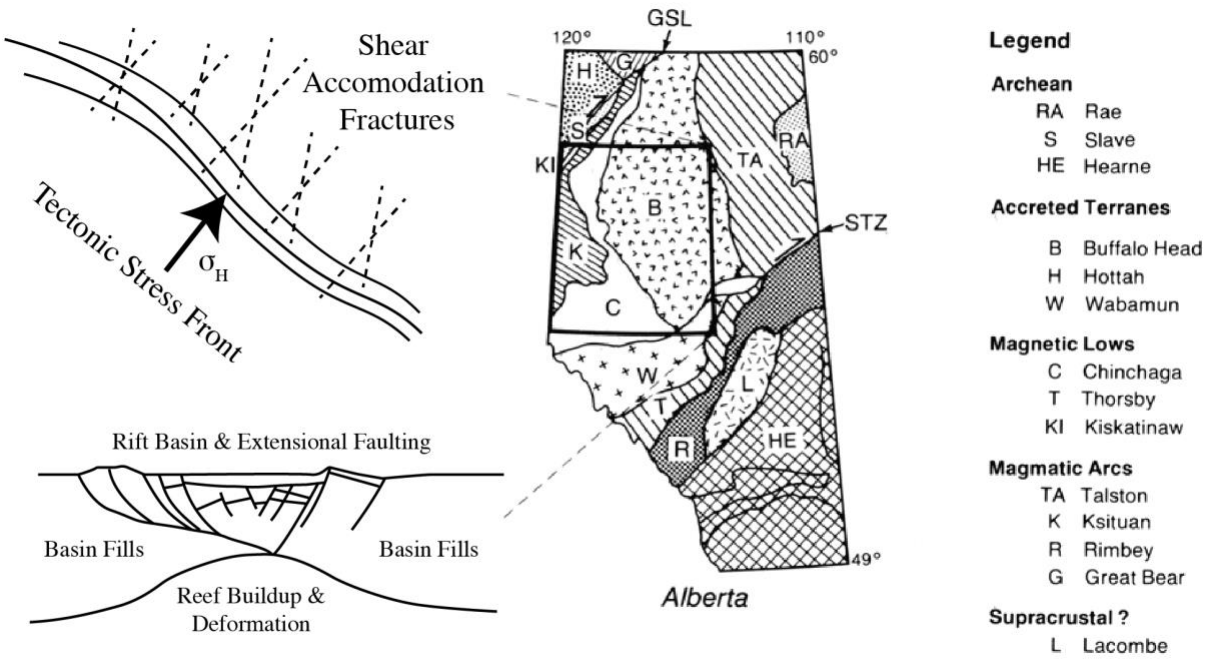

Figure 4. An illustration of the faulting theories presented in this paper. The upper left cartoon shows the formation of oblique shear accommodation fractures during tectonic mountain building. The lower cartoon shows a typical extensional faulting regime that might have resulted from the presence of the Chinchaga rift basin in combination with reef building and resultant deformation. The location of Chinchaga basin (C) is illustrated in the right panel, after O'Connell *et al.* (1990).

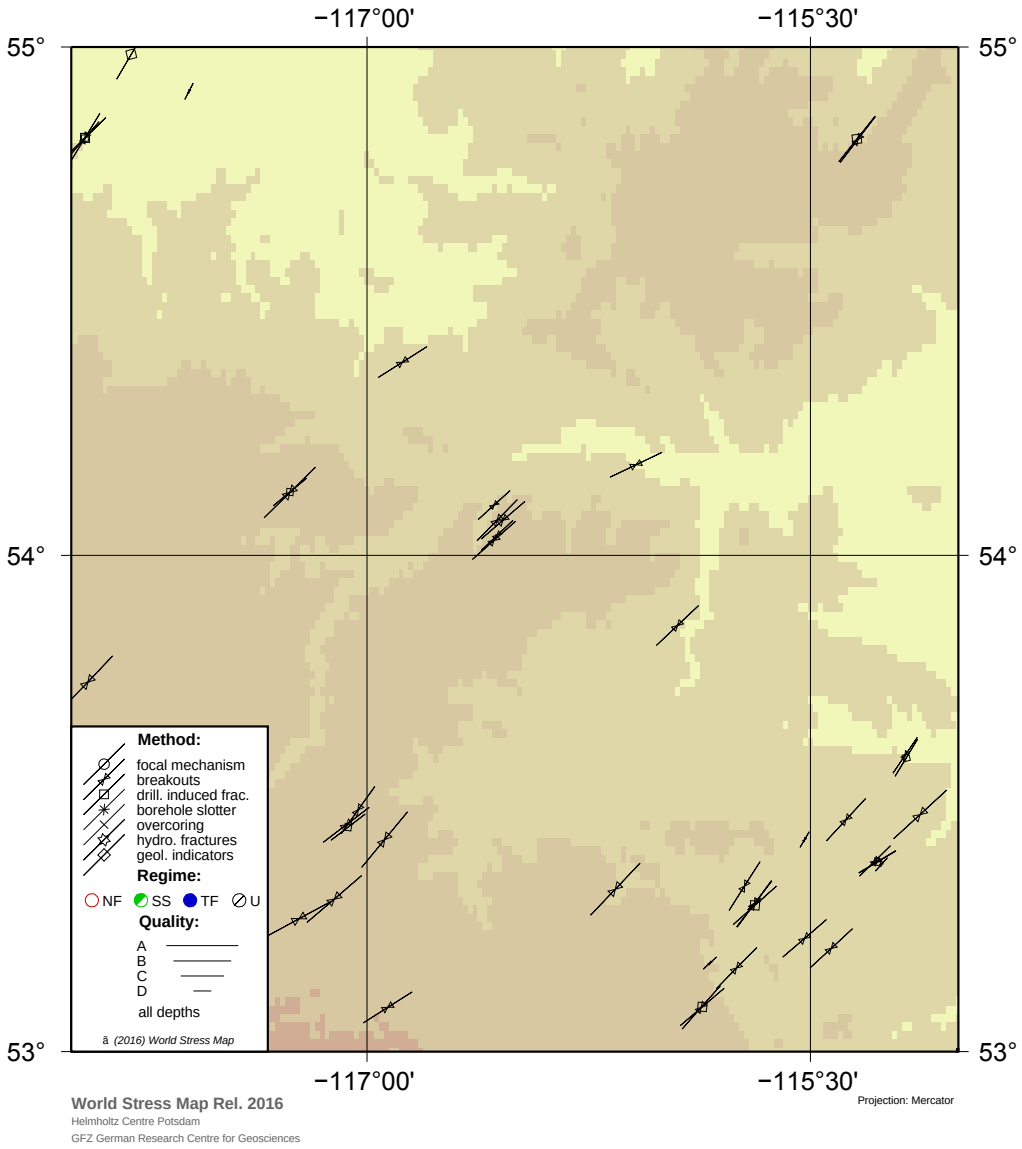

Figure 5. An excerpt of the world stress map showing interpreted borehole breakouts and DFITs in the Kaybob area of the Duvernay (Heidbach et al., 2008).

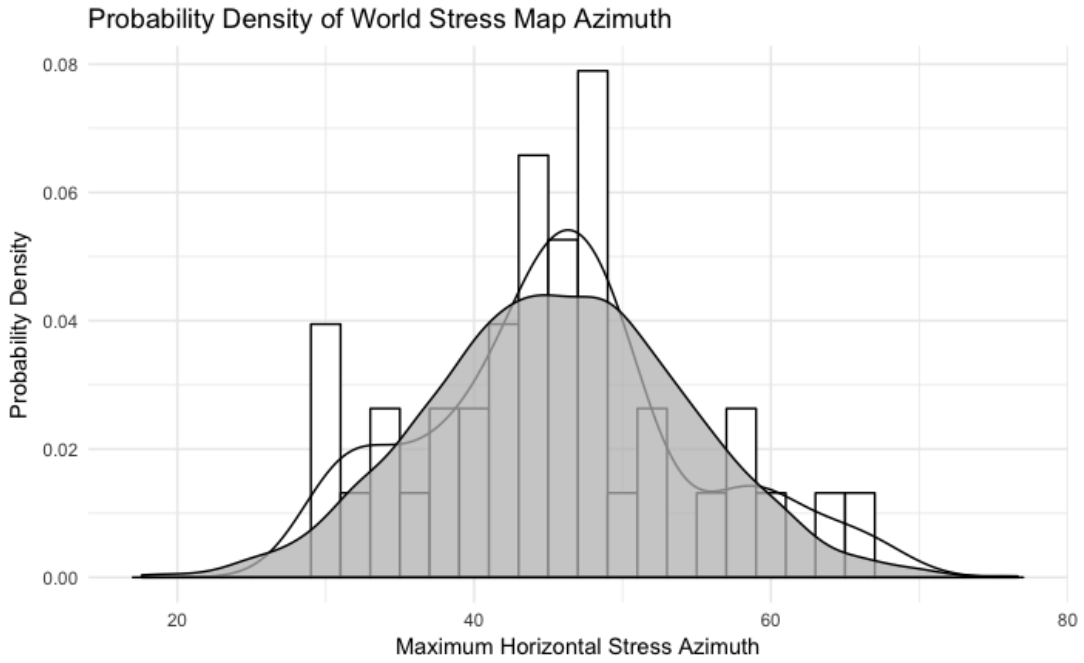

Figure 6. A distribution (normalized probability mass function) and interpreted distribution (probability density function) of the horizontal stress azimuths in the Kaybob area of the Duvernay, which are illustrated in Figure 5 and obtained from Heidbach et al. (2008).

Table 1. Summary of the inputs used in the Monte-Carlo analysis of fault slip potential, listing the type of probability distribution, the shape or mean parameter (which usually defines the centre of the distribution), and the scale parameter (which usually defines the spread or variance of the distribution). See Hajati *et al. 2015* and Fenton and Griffiths (2008), among others, for further details.

Parameter	Distribution	Shape / Mean	Scale
Depth (m)	Single Value	3,400	-
Horizontal Stress Azimuth (°)	Normal	45.7	8.9
c (MPa)	Exponential	-	1
σ_V (MPa)	Normal	22.6	0.25
σ_H (MPa)	Normal	29.5	0.75
σ_h (MPa)	Normal	21.0	0.5
u (MPa)	Gamma	264	16
Fault Strike (°)	Uniform	0 / 45	-
Fault Friction (°)	Gamma	150	250
Pressure Perturbation (MPa)	Exponential	-	0.5
σ_H Perturbation (MPa)	Exponential	-	10

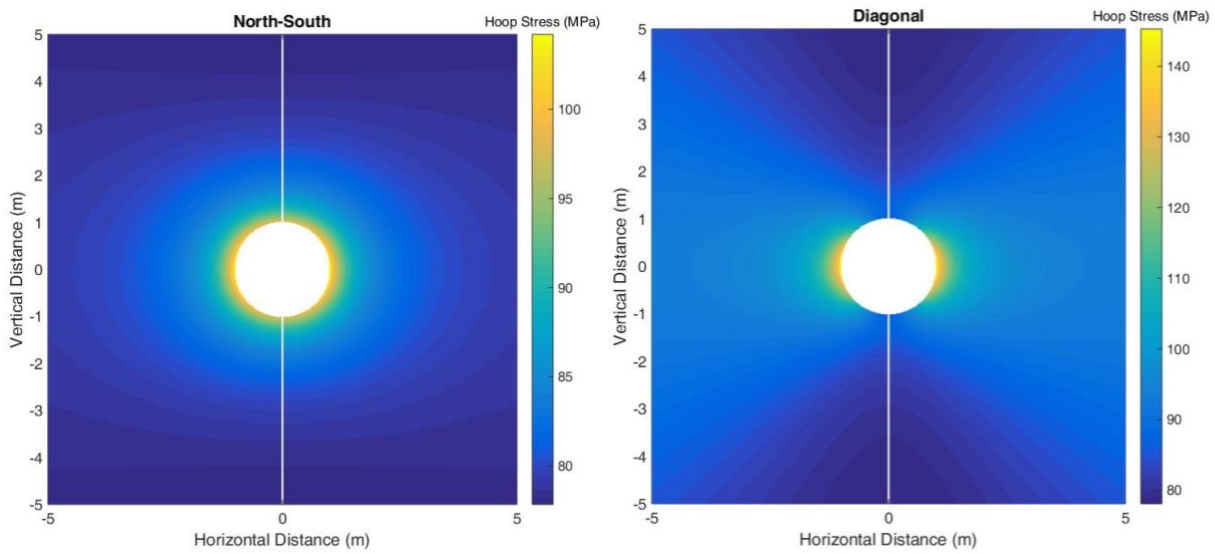

Figure 7. A plot of hoop stress around a north-south lateral (left) and diagonal lateral (right). The colour scale shows the hoop stress in MPa. Stress concentrations are clearly visible in the diagonal lateral.

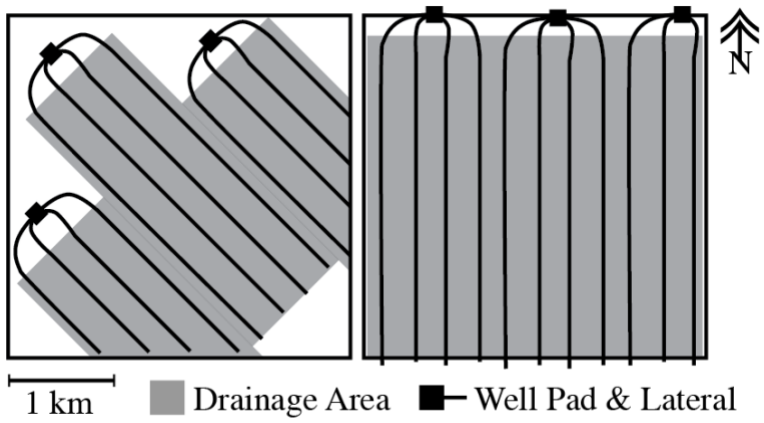

Figure 8. A scaled illustration showing the development of a four-section leasehold. The diagonal completion strategy is shown on the left and the north south on the right.

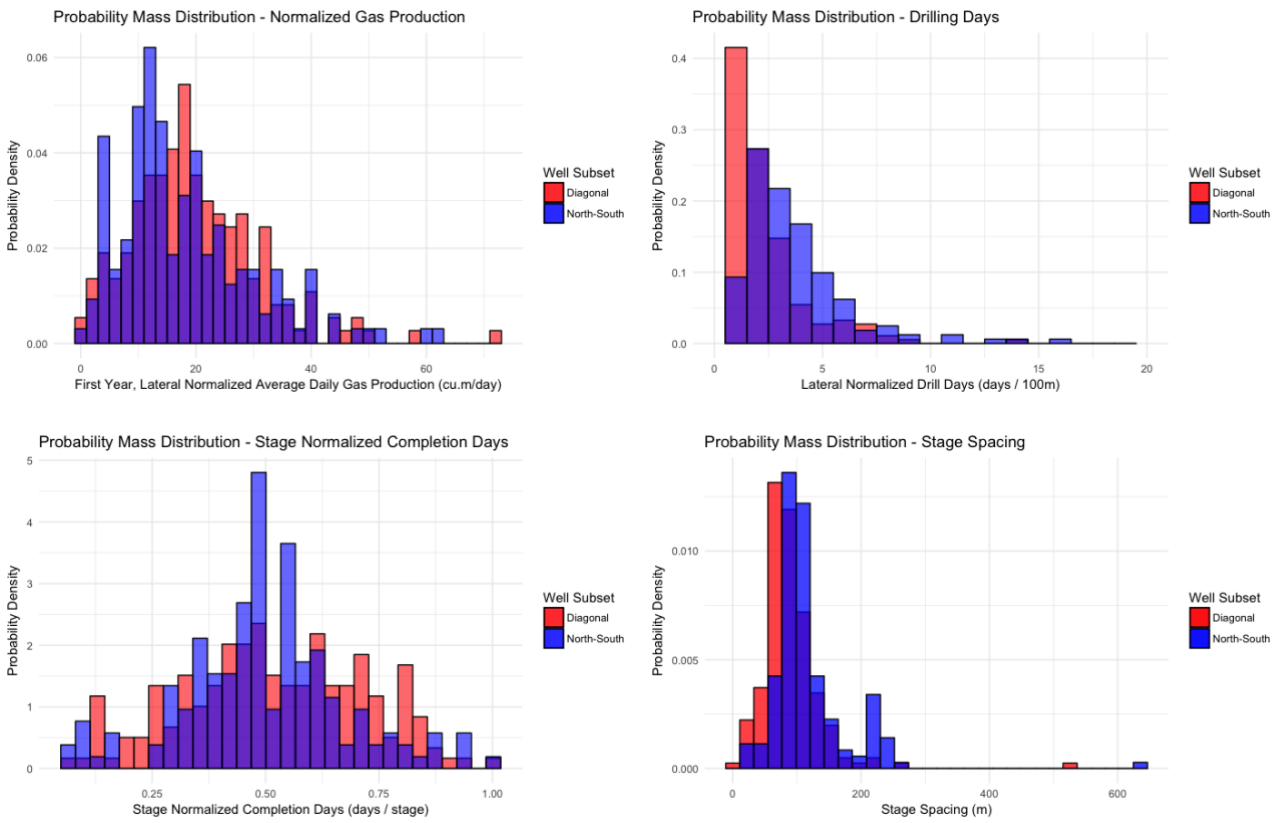

Figure 9. Histograms of the four comparisons of north south (blue) and diagonal (red) wells. A histogram of lateral normalized gas production is shown in the upper left. A histogram of lateral normalized drilling days is shown in the upper right. A histogram of stage spacing normalized completions days is shown the bottom left. A histogram of stage spacing is shown in the bottom right.

Acknowledgements:

The work presented here is part of a research project supported by the Canada First Research Excellence Fund (CFREF), the Microseismic Industry Consortium (MIC), and the ReDevelop program. The authors thank Dr. Dave Eaton, Dr. Ron Wong, Dr. Jeff Priest, and Dr. Celia Kennedy for their technical guidance. The advice of Dr. Schultz was invaluable in scoping out this project. Matt Graham of Vesta Energy Ltd. provided detailed guidance for the comparison of north south vs. diagonal laterals.

Literature Cited:

Aguilera, R., 1995. *Naturally fractured reservoirs*, Tulsa, OK: Pennwell Publishing Company.

Atkinson, G.M. et al., 2016. Hydraulic fracturing and seismicity in the Western Canada Sedimentary Basin. *Seismological Research Letters*, 87(3), pp.631–647.

Brune, J.N., 1970. Tectonic stress and the spectra of seismic shear waves from earthquakes. *Journal of geophysical research*, 75(26), pp.4997–5009.

Dunn, L. et al., 2012. The Duvernay Formation (Devonian): Sedimentology and Reservoir Characterization of a Shale Gas / Liquids play in Alberta, Canada. In *GeoConvention 2012: Vision*. Calgary: Canadian Society of Petroleum Geologists, p. 5.

Ellsworth, W.L., 2013. Injection Induced Earthquakes. *Science*, 341(6142), pp.1225942–1225942.

Farahbod, A.M. et al., 2015. Investigation of regional seismicity before and after hydraulic fracturing in the Horn River Basin, northeast British Columbia. *Canadian Journal of Earth Sciences*, 52(2), pp.112–122.

Fox, A.D. & Soltanzadeh, M., 2015. A Regional Geomechanical Study of the Duvernay Formation in. , pp.1–4.

Hajati, T., Langenbruch, C. & Shapiro, S.A., 2015. A statistical model for seismic hazard assessment of hydraulic-fracturing-induced seismicity. *Geophysical Research Letters*, 42(24), pp.10601–10606.

Healy, J.H. et al., 1968. The Denver Earthquakes. *Science*, 161(3848), pp.1301–1310.

Heidbach, O. et al., 2010. Global crustal stress pattern based on the World Stress Map database release 2008. *Tectonophysics*, 482(1–4), pp.3–15.

Hiramatsu, Y. & Oka, Y., 1962. Analysis of stress around a circular shaft or drift excavated in ground in a three dimensional stress state. *Journal of Mining and Metallurgy Institute of Japan*, 78, pp.93–98.

Hitzman, M.W., 2012. *Induced Seismicity Potential in Energy Technologies*,

Hubbert, M.K. & Willis, D.G., 1957. Mechanics of hydraulic fracturing. *Transactions of Society of Petroleum Engineers of AIME*, 210, pp.153–169.

Jaeger, J.C., 1959. The frictional properties of joints in rock. *Geofisica Pura e Applicata*, 43(1), pp.148–158.

Kirsch, C., 1898. Die theorie der elastizitat und die bedurfnisse der festigkeitslehre. *Zeitschrift des Vereines Deutscher Ingenieure*, 42, pp.797–807.

Labuz, J.F. & Zang, A., 2012. Mohr Coulomb failure criterion. *Rock Mechanics and Rock Engineering*, 45, pp.975–979.

Lele, S.P. et al., 2017. Geomechanical Analysis of Hydraulic Fracturing Induced Seismicity at Duvernay Field in Western Canadian Sedimentary Basin. , pp.1–5.

Massey Jr, F.J., 1951. The Kolmogorov-Smirnov test for goodness of fit. *Journal of the American statistical Association*, 46(253), pp.68–78.

Maxwell, S.C. et al., 2009. Fault activation during hydraulic fracturing. *SEG Technical Program Expanded Abstracts 2009*, (June 2010), pp.1552–1556. Available at: http://library.seg.org/doi/abs/10.1190/1.3255145.

Mohr, O., 1900. Welche umstände bedingen die elastizitätsgrenze und den Bruch eines materials. *Zeitschrift des Vereins Deutscher Ingenieure*, 46(1524–1530), pp.1572–1577.

Nelson, R., 2001. *Geologic analysis of naturally fractured reservoirs*, Gulf Professional Publishing.

O'Connell, S.C., Dixon, G.R. & Barclay, J.E., 1990. The origin, history, and regional structural development of the Peace River Arch, Western Canada. *Bulletin of Canadian Petroleum Geology*, 38A, pp.4–24. Available at: http://archives.datapages.com/data/cspg/data/038a/038a001/0004.htm.

Raleigh, C.B., Healy, J.H. & Bredehoeft, J.D., 1976. An experiment in earthquake control at rangely, colorado. *Science (New York, N.Y.)*, 191(4233), pp.1230–1237. Available at: http://www.ncbi.nlm.nih.gov/pubmed/17737698.

Richter, C.F., 1935. An instrumental earthquake magnitude scale. *Bulletin of the Seismological Society of America*, 25, pp.1–32.

Rivard, C. et al., 2014. An Overview of Canadian Shale Gas Production and Environmental Concerns. *International Journal of Coal Geology*, 126, pp.64–76.

Schultz, R. et al., 2015. Hydraulic fracturing and the Crooked Lake Sequences: Insights gleaned from regional seismic networks. *Geophysical Research Letters*, 42, pp.2750–2758.

Soltanzadeh, M. et al., 2015. Application of Mechanical and Mineralogical Rock Properties to Identify Fracture Fabrics in the Devonian Duvernay Formation in Alberta. *Proceedings of the 3rd Unconventional Resources Technology Conference*, (Cdl), pp.1–14. Available at: http://search.datapages.com/data/doi/10.15530/urtec-2015-2178289.

Soltanzadeh, M. et al., 2015. A Regional Review of Geomechanical Drilling Experience and Problems in the Duvernay Formation in Alberta. , (Cdl), pp.1–11.

Wright, G.N. et al., 1994. Structure and architecture of the Western Canada sedimentary basin. *Geological atlas of the Western Canada sedimentary basin*, 4, pp.25–40.

Zoback, M.D., 2010. *Reservoir Geomechanics*, Cambridge, U.K.: Cambridge University Press.